Effect of Molecular Weight between Crosslinks on the Fracture Behavior of Rubber-Toughened Epoxy Adhesives

BYOUNG UN KANG,[1] JAE YOUNG JHO,[1] JUNKYUNG KIM,[2] SANG-SOO LEE,[2] MIN PARK,[2] SOONHO LIM,[2] CHUL RIM CHOE[2]

[1] School of Chemical Engineering, Seoul National University, Seoul 151-742, Korea

[2] Polymer Hybrids Research Center, Korea Institute of Science and Technology, 39-1 Hawolgok-dong, Sungbuk-gu, Seoul 136-791, Korea

Received 21 November 1999; accepted 4 February 2000

ABSTRACT: The effect of molecular weight between crosslinks, M_c, on the fracture behavior of rubber-toughened epoxy adhesives was investigated and compared with the behavior of the bulk resins. In the liquid rubber-toughened bulk system, fracture energy increased with increasing M_c. However, in the liquid rubber-toughened adhesive system, with increasing M_c, the locus of joint fracture had a transition from cohesive failure, break in the bond layer, to interfacial failure, rupture of the bond layer from the surface of the substrate. Specimens fractured by cohesive failure exhibited larger fracture energies than those by interfacial failure. The occurrence of transition from cohesive to interfacial failure seemed to be caused by the increase in the ductility of matrix, the mismatch of elastic constant, and the agglomeration of rubber particles at the metal/epoxy interface. When core-shell rubber, which did not agglomerate at the interface, was used as a toughening agent, fracture energy increased with M_c. © 2000 John Wiley & Sons, Inc. J Appl Polym Sci 79: 38–48, 2001

Key words: rubber-toughened epoxy adhesive; formulation; interfacial failure; rubber agglomeration

INTRODUCTION

Epoxy resin is being used as the most common structural adhesive by virtue of its high cohesive and adhesive strength, low shrinkage, and versatility in formulating and processing. Cured epoxy resin, however, has a brittle nature with poor resistance to crack growth. As a result, it is frequently toughened by the incorporation of a rubbery phase for applications. When toughening is considered, it is known that plastic deformation of the epoxy matrix is mostly responsible for the toughening effect in rubber-toughened epoxies. The plastic deformation, which is induced by rubber particles, can be divided into shear yielding of epoxy matrix between the neighboring rubber particles and plastic void growth of epoxy matrix surrounding the particles. Yee and Pearson[1] identified that the role of the rubber particles in the toughening is to relieve the constraint in front of the crack tip by rubber cavitation, and trigger for the formation of shear bands. Also, the quantitative modeling by Huang and Kinloch[2] revealed the importance of plastic void growth as well as matrix shear deformation in epoxy toughening.

Although the addition of various rubber particles has effectively enhanced the toughness of bulk epoxy resins, epoxy adhesives have not been toughened effectively.[1–9] The reason, for the most part, is that the toughening mechanisms that

Correspondence to: J. Kim (jkkim@kistmail.kist.re.kr).

Journal of Applied Polymer Science, Vol. 79, 38–48 (2001)

functioned in bulk did not work in adhesives. Observed results initially by Bascom et al.,[3] and subsequently by other researchers[4–7] have demonstrated the complex effect of bond thickness on the fracture energy of a rubber-toughened epoxy. On the assumption that all other factors are equal, it was proposed that increased constraint brought about by a reduction in bond thickness could produce an extension of the crack tip plastic zone along the adhesive length. According to their proposition, the extended plastic zone can increase the toughness of the adhesive, and consequently affect the adhesive fracture energy. Bell and Kinloch[8] noted that the value of the adhesive fracture energy may be dependent on the type of substrates used, even when cohesive fracture through the adhesive layer is observed. They elucidated that such a dependence arises from the transverse modulus of the substrate, which influences the form of the stress field ahead of the crack in the adhesive layer. In summary, in addition to the factors governing the fracture of bulk epoxies, it appeared that other factors, as mentioned above, like the thickness of adhesive layer,[3–7] the type and surface treatment of substrate[8,9] affected the fracture behavior of adhesive system.

It was supposed that the variation of adhesive properties with formulation is another influential parameter on adhesive fracture. Many researchers have shown that the extent of fracture energy enhancement in a rubber-toughened epoxy depends on the crosslink density of the epoxy resins.[10,11] Pearson and Yee[10] suggested that the fracture toughness of the rubber-toughened epoxies is a relatively strong function of the molecular weight, and the toughenability of a diglycidyl ether bisphenol A (DGEBA)-based epoxy resin by rubber addition depends on the crosslink density of the epoxy matrix. They defined that toughenabilty is related to the ability of epoxy to undergo plastic deformation in applied stress states, i.e., the lower the crosslink density, the greater the toughenability. Recent study by Kishi et al.[11] provided a detailed description of the effect of the matrix properties on fracture energy. It was proposed that the lower elastomer toughenability of highly crosslinked networks could be a consequence of their low intrinsic ductility.

The purpose of this study was to have a more systematic understanding of how the adhesive fails according to the ductility change of epoxy resin. In this study, with fixed adhesive thickness and other conditions, molecular weight between crosslinks, M_c, of epoxy resin was varied by using different epoxy equivalent weights (EEW) of DGEBA-based epoxy prepolymer, and the fracture behavior of adhesives was investigated. Additionally, another goal was to evaluate the role of the rubber particles on the adhesive fracture process compared with bulk fracture.

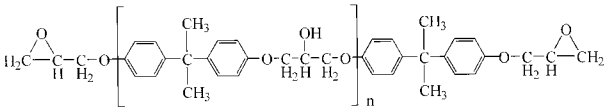

(a) Diglycidyl ether of bisphenol A (DGEBA) - epoxy

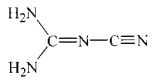

(b) dicyandiamide (DICY)

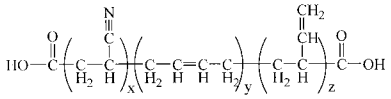

(c) carboxyl-terminated butadiene-acrylonitrile copolymer (CTBN)

Figure 1 The chemical structures of the materials. (a) Diglycidyl ether of bisphenol A (DGEBA; Kukdo Chemical Co.) epoxy; (b) dicyandiamide (DICY; Aldrich Chemical Co.); and (c) carboxyl-terminated butadiene-acrylonitrile copolymer (Hycar®, BF Goodrich).

EXPERIMENTAL

Materials

DGEBA epoxy prepolymers with three different EEW and dicyandiamide (DICY) were obtained from Kukdo Chemicals and Aldrich, respectively. Two types of carboxyl-terminated butadiene-acrylonitrile copolymer (CTBN), a Hycar®; liquid rubber, were obtained from BF Goodrich and designated as CTBN8 [17 wt % acrylonitrile (AN) content] and CTBN13 (27 wt % AN content) according to the supplier's instruction. The core-shell rubber, prepared in our laboratory, consisted of polybutylacrylate core crosslinked with triallyl isocyanate and polymethylmethacrylate shell crosslinked with divinyl benzene (core/shell = 50:50 by weight). The predetermined size of the core-shell rubber particles was about 630 nm. The chemical structures of materials used are shown in Figure 1.

Table I Recipe of Cured Bulk Specimens

Code	DGEBA-Type Epoxy (g)	EEW (g/eq)	DICY (g)	Azine (g)	Rubber (g)
E1	120	184–190	8.09	0.21	19.17
E2	120	450–500	3.18	0.06	18.41
E3	120	900–1000	1.59	—	18.20

Preparation Procedures

The stoichiometric amount of the hardener accorded to previous studies,[12,13] and the formulations for the bulk and the adhesives are listed in Table I. Because of several types of epoxy equivalent weights of the resins used, and the corresponding viscosity change, three kinds of cure procedure were used for the preparation of the specimens as shown in Table II. Details of these procedures are as follows. First the DGEBA epoxy and rubber mixture were heated to viscous melt and degassed for less than an hour. After the vacuum was removed, the hardener DICY and the catalyst azine were added to the epoxy/rubber mixture while stirring slowly. Some of the mixture was again degassed and poured into a Teflon-coated mold to prepare the bulk specimens, and the other portion was coated on bonding surface of the substrates, i.e., the tapered double cantilever beam (TDCB) specimens pretreated according to ASTM D2651, that were preheated at cure temperature. In the case of the TDCB specimens, the Kapton® film was used as constant thickness spacer as well as preinserted notch. The specimens were allowed to react at cure temperature for 2 h and postcure for 20 min at 220°C in an air-circulating oven. After that, the specimens were allowed to cool slowly to room temperature.

Aluminum alloy 6061 was used as the substrate material, blocks of which were machined according to ASTM D3433. To ensure good adhesion of the adhesives, the surfaces to be jointed had to be cleaned according to ASTM D2651 before the adhesion was applied. The substrate was polished down to 0.3 μm using alumina powder, cleaned with acetone/water, chemically etched in a bath of sodium dichromate/sulfuric acid/distilled water (3:10:30 by weight) at 70°C for 15 min, washed with water, and dried.

Table II Conditions for the Preparation of the Epoxy Resins

		Temperature and Time (°C, min)		
Code	EEW	Mixing and Degassing	Cure	Postcure
E1	184–190	80, 60	120, 120	220, 20
E2	450–500	100, 40	120, 120	220, 20
E3	900–1000	>160, 30	160, 120	220, 20

Tests and Measurements

Glass transition temperature (T_g) of the cured epoxies was determined with a Perkin-Elmer DSC-7 at the heating rate of 10°C/min. Equilibrium modulus of the resins in their rubbery state was measured with a dynamic mechanical thermal analyzer (Rheometrics MK-II DMTA) in the bending mode at a frequency of 1 Hz. Young's modulus and yield stress were determined by uniaxial compression test using a universal testing machine (Instron 4201 UTM) run at a crosshead speed of 1.3 mm/min. Specimens for the compression test were machined to the dimension of 4, 4, and 8 mm in width, breadth, and length, respectively.

Number average molecular weight between crosslinks, M_c, was determined using the equation from the rubber elasticity theory[14]:

$$M_c = q\,\frac{\rho RT}{G_c}$$

where q is the front factor (usually 1), ρ is the density, R is the gas constant, and T is the temperature. G_c is the equilibrium modulus in the rubbery region that was determined by the DMTA measurement.

Critical strain energy release rate or fracture energy, G_{Ic}, of bulk resin was determined from single-edge notched three-point bending (SEN-3PB) tests and the following equation[15]:

$$W = G_{Ic} \times BD\Phi$$

where W is the stored elastic energy up to the point of fracture, B is the sample thickness, D is

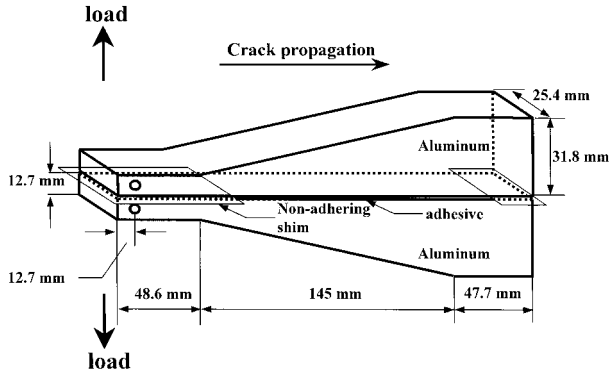

Figure 2 Schematic diagram of the tapered double cantilever beam (TDCB) specimen geometry.

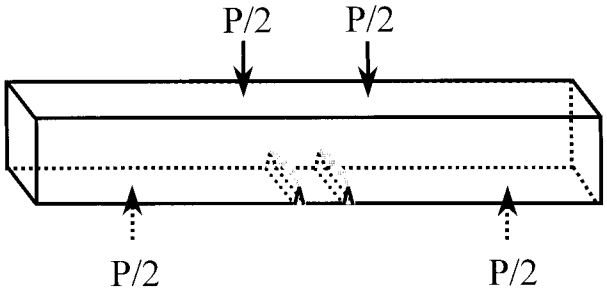

Figure 3 Schematic diagram of the double-notched four-point bending (DN-4PB) specimen geometry.

the width. G_{Ic} is obtained from the slope in the plot of W as a function of $BD\Phi$, when the geometry dependence, Φ, is given by the equation, $\Phi = (a/2D) + (L/9\pi a)$. For each measurement, seven to ten specimens were machined to the dimension of 100 × 4 (B) × 11 (D) mm^3, and tested with a span length (L) of 33 mm and varying initial crack length (a). The specimens were loaded to failure in the UTM run at a constant crosshead speed of 1.3 mm/min and room temperature.

Fracture energy of the adhesive layers was determined through Mode I fracture test of TDCB specimens, following the procedure described in ASTM D3433.[5,7,16] Epoxy resin with the thickness of ca. 150 μm, cured between the metal blocks with the geometry shown in Figure 2, were tensioned to failure with a UTM at a crosshead speed of 1.3 mm/min at room temperature. G_{Ic} was calculated from the following equation:

$$G_{Ic} = \frac{4P_c^2 m}{b^2 E}$$

where P_c is the critical load for crack initiation, b is the specimen width, E is the tensile modulus of the substrate, and m is the constant determined by the geometry of specimen, which is 3.54 mm^{-1} for this geometry.

Microscopic Observation

The subsurface deformation zones of the tested specimens were observed using an optical microscope (Nikon Optiphot 2-pol) in the transmitted light mode. The bulk specimens were fractured by using the double-notched four-point bending (DN-4PB) test,[17] and the well-developed damage zones that represent the conditions prior to the failure of the bulk epoxy were investigated. Figure 3 is a schematic representation showing details of the test. Sections taken from the tested bulk and adhesive specimens in the direction parallel to the crack propagation, perpendicular to the fracture surface, were ground and polished to thin sections using the petrographic polishing technique.[17,18] The fracture surfaces of the SEN and the TDCB specimens were characterized by scanning electron microscope (Hitachi S 2500S) at an accelerating voltage of 10 kV after sputtering with a gold-palladium coating.

RESULTS AND DISCUSSION

Characteristics of the Epoxies

T_g, yield stress (σ_y), and modulus (E) of the neat resins are summarized with their M_c in Table III. As shown in Figure 4, dynamic mechanical thermal analysis of epoxy resins revealed that T_g and rubbery plateau modulus (E'), decreased with increasing epoxy equivalent weight of prepolymer. The decrease in the dynamic mechanical properties was attributed to the more unrestricted motion of chain segments responsible for the damping with increasing M_c. As a result, the resin with

Table III Thermal and Compressive Mechanical Properties of the Cured Neat Epoxy Resins

Code	M_c	T_g (°C)	σ_y (MPa)	E (GPa)
E1	456	139.1	116.7	2.68
E2	1600	110.4	96.2	2.61
E3	2237	103.6	87.9	2.34

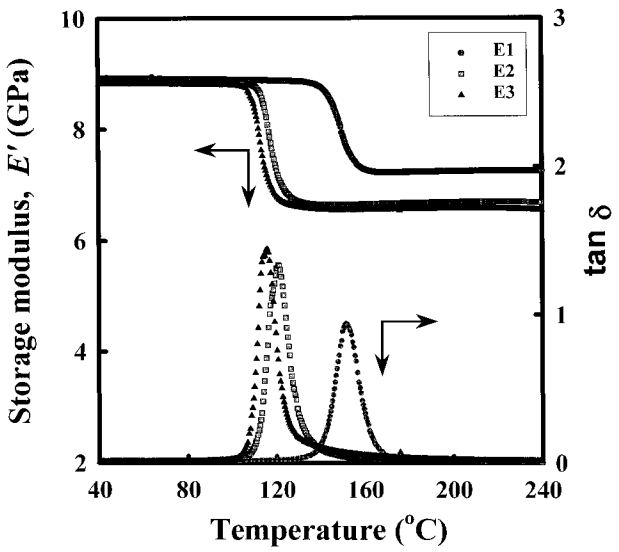

Figure 4 Dynamic mechanical thermal analysis of neat epoxies.

higher M_c appeared to be softer, showing lower thermal and mechanical properties.

Morphological Behavior of Rubber-Toughened Epoxies

Figure 5 shows the optical micrographs of the thin sections taken parallel to the crack propagation direction for DN-4PB specimens, and Figure 6 reveals scanning electron micrographs taken from the fracture surface of SEN-3PB specimens. In case of the same matrix systems, especially in the matrix type of E2, the rubber particles in the CTBN8/E2 system [see Figs. 5(b) and 6(b)] had larger size than those in the CTBN13 system [see Figs. 5(c) and 6(c)]. In DGEBA-based epoxy/CTBN rubber blends, it has been well known that the phase separation is facilitated by the increase in molecular weight of epoxy and the variation of

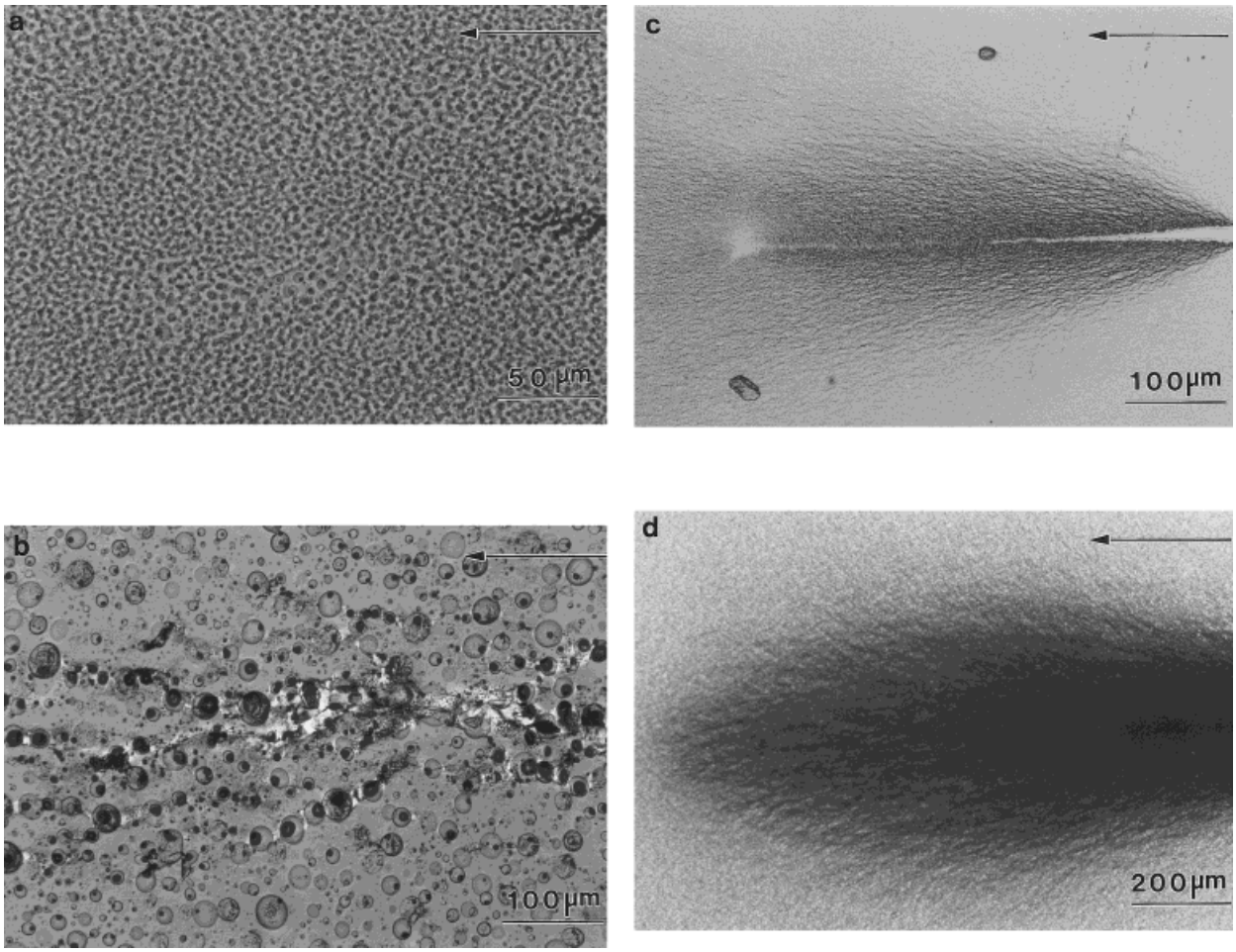

Figure 5 Transmission optical photomicrographs of thin sections taken mid plane near the crack tip of the DN-4PB specimens: (a) E1/CTBN8; (b) E2/CTBN8; (c) E2/CTBN13; and (d) E3/CTBN13. Arrows indicate the direction of crack propagation.

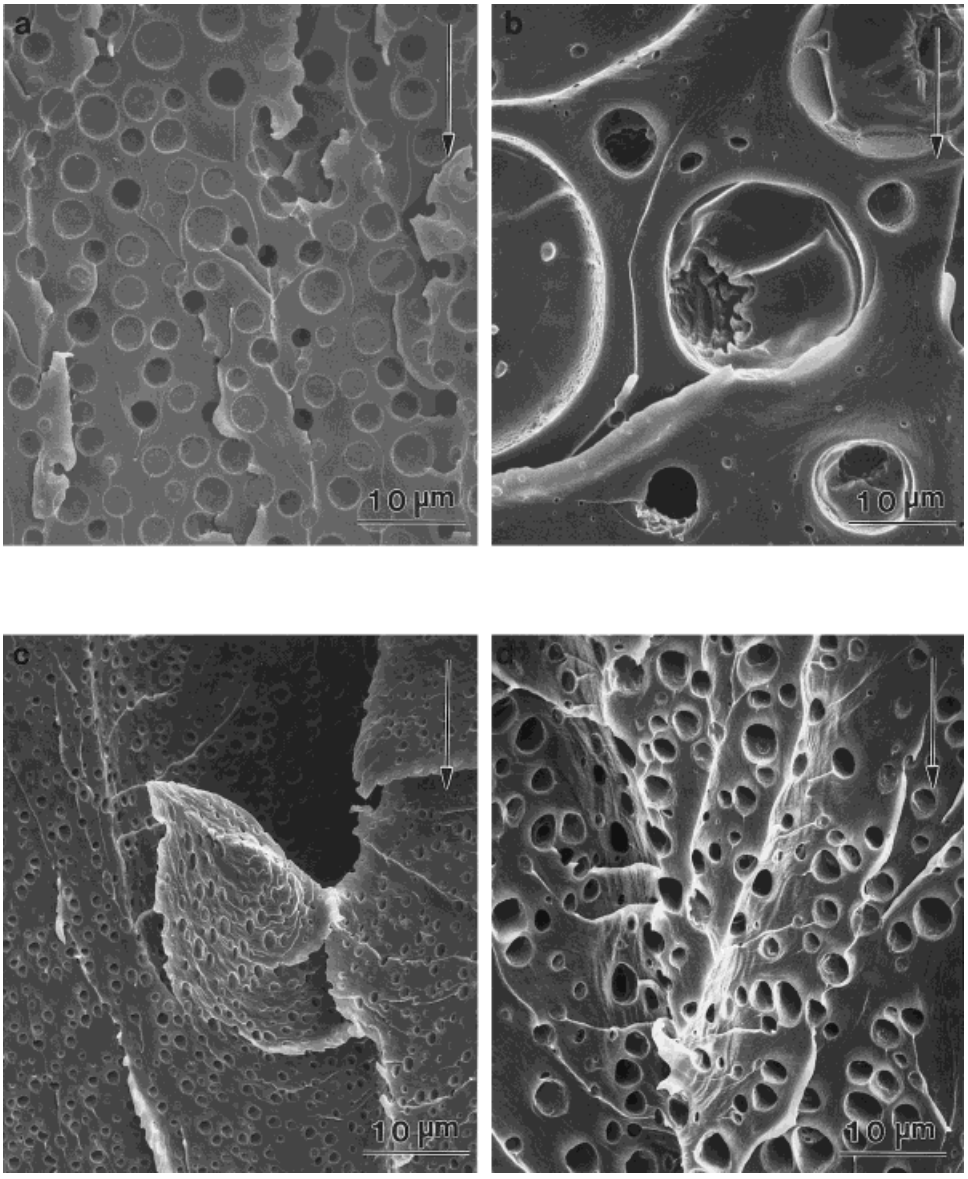

Figure 6 Scanning electron micrographs of the fracture surfaces of the SEN-3PB specimens: (a) E1/CTBN8; (b) E2/CTBN8; (c) E2/CTBN13; and (d) E3/CTBN13. Arrows indicate the direction of crack propagation.

solubility parameter that occurs during cure reaction.[19,20] On the other hand, the increase in the AN content of a CTBN rubber was reported to improve the compatibility between the CTBN rubber and the epoxy.[21,22] It was explained by the decrease in the difference between the solubility parameters of both components (20.9, 18.7, and 17.9 $MPa^{1/2}$ for DGEBA epoxy, CTBN13, and CTBN8, respectively) with increasing the AN content. In this study, the mixture of an epoxy with CTBN13 of high AN content (27 wt %), compared with CTBN8 (17 wt %), showed a retardation of phase separation, resulting in a reduction of rubber particle size.

In the case of the same toughener systems, Figures 5 and 6 show that an increase in M_c from E1 to E2 with CTBN8, or from E2 to E3 with CTBN13 resulted in increasing rubber particle size. Previous study on the miscibility of epoxy/rubber mixture by Verchere et al.[22] showed that the miscibility gap in epoxy/rubber mixture increased with an increase in the molecular weight of the epoxy prepolymers. Therefore, it has become obvious that the miscibility of epoxy mono-

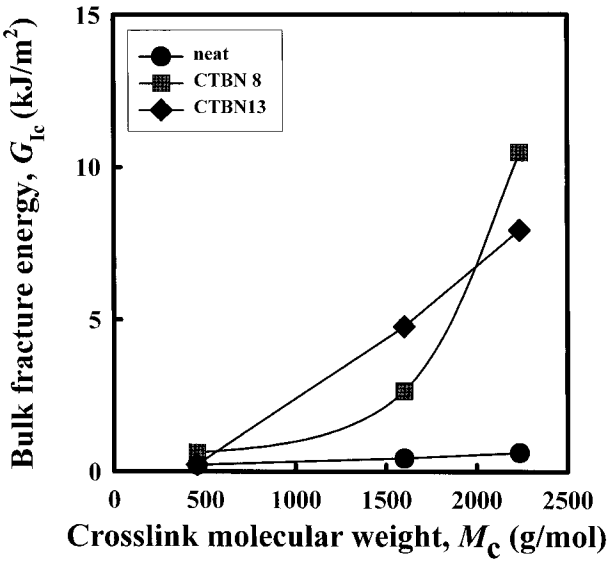

Figure 7 Bulk fracture energy of rubber-toughened epoxies.

mers with a rubber is very sensitive to the molecular weight of the epoxy prepolymer.

In the epoxy/CTBN mixture investigated, consequently, an increase in AN content (from CTBN8 to CTBN13) or a decrease in M_c (from E3 to E1) resulted in the decrease in size of rubber particles.

Fracture Behavior of Rubber-Toughened Bulk Epoxies

Figure 7 shows that fracture energy of the CTBN-toughened bulk epoxy increased with increasing M_c, whereas that of neat epoxy was little changed. The behavior has been commonly observed in many toughened epoxy systems. The dominant mechanisms for rubber toughening of epoxies, proposed by many researchers,[1,2,10,17,20] are the cavitation of rubber particles and cavitation-induced plastic deformation of epoxy matrix such as shear and dilatational deformations. As M_c of the epoxy matrix increased, the fracture energy of the toughened epoxy increased because of the enhanced ability of matrix to deform.[10,11] In neat epoxy resin, where rubber particles were absent and the corresponding rubber cavitations were not available, the enhanced ductility alone could not effectively enhance fracture energy.

Whereas G_{Ic} of CTBN13-toughened epoxy increased linearly, the increment of CTBN8-toughend epoxy negatively deviated from the linearity line. The low G_{Ic} value of E2/CTBN8 could be explained by the presence of particles as large as several tens of micrometers [Figs. 5(b) and 6(b)]. It is generally known that rubber particles larger than a few micrometers are not effective in epoxy toughening.[17] Still, G_{Ic} of E2/CTBN8 is larger than that of E1/CTBN8 due to the enhanced ductility or toughenability of epoxy matrix by rubber addition, which was mentioned previously. The broad, actually close to bimodal, distribution in particle size of E2/CTBN8 was thought to contribute to enhancing fracture energy. Stress field formed by early-stressed larger particles might have enhanced the cavitations of smaller neighbors, which has been reported previously in epoxy toughening.[17,20] The complicated pattern of shear yielding observed in deformation zone of E2/CTBN8 of Figure 5(b) was considered supportive of this explanation.

Fracture Behavior of Rubber-Toughened Epoxy Adhesives

It was found that the fracture behavior of neat epoxy adhesives followed cohesive failure mode, and G_{Ic} increased linearly as seen in Figure 8, which was quite similar to that of neat bulk resin. However, this was not the case in toughened adhesives. For CTBN8-toughened adhesive system, fracture energy decreased with the increase in M_c. It is believed to be caused by the transition in the fracture mode from cohesive (E1/CTBN8) to

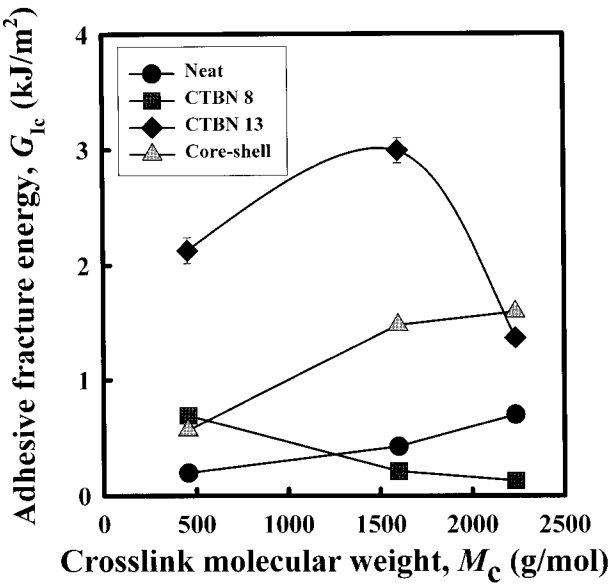

Figure 8 Adhesive fracture energy of rubber-toughened epoxies.

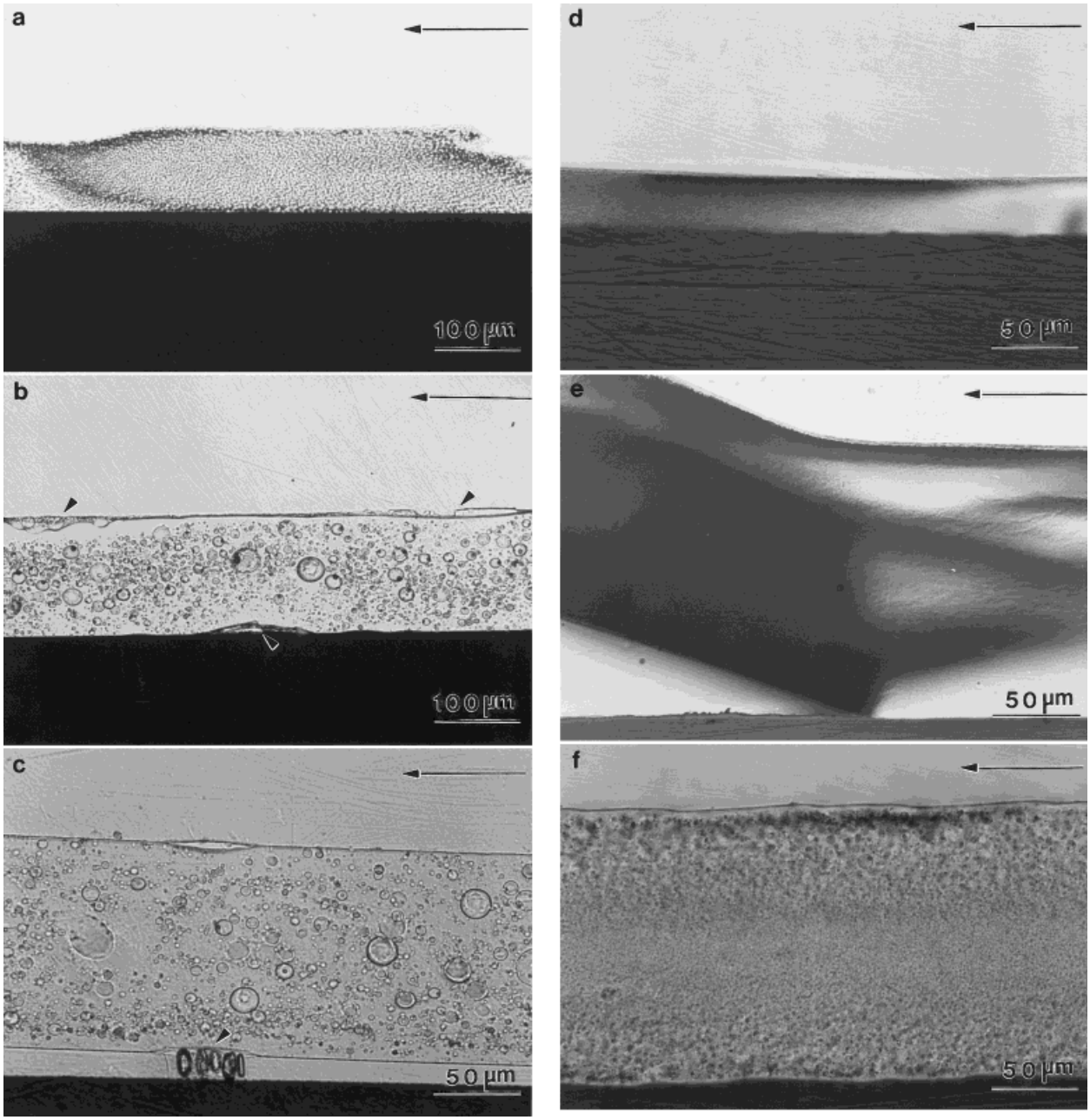

Figure 9 Optical photomicrographs, taken under cross-polarized light, of the region below the fracture surfaces of the TDCB specimens: (a) E1/CTBN8; (b) E2/CTBN8; (c) E3/CTBN8; (d) E1/CTBN13; (e) E2/CTBN13; and (f) E3/CTBN13. Arrows indicate the direction of crack propagation. Wedges indicate the agglomeration of rubber particles.

interfacial failure (E2/CTBN8). As shown in Figure 9(b,c), the rubber particles did not cavitate in the specimens that failed at the interface between the resin and substrate, in contrast to that which failed cohesively [Fig. 9(a)] and to that in bulk specimen [Fig. 5(b)].

G_{Ic} of CTBN13-toughened epoxy adhesives exhibited a maximum when M_c was about 1600 (E2). In this specimen, a larger and through-thickness type of deformation zone [Fig. 9(e)], compared with E1/CTBN13 [Fig. 9(d)], was observed. Despite the inhomogeneity of deformation zone in adhesive layer, plastic wake, i.e., the trace of the deformation zone, was observed to farther extend along the length of the adhesive layer (not fully shown here). As M_c further increased (from

Table IV Mechanical Properties of the Rubber-Toughened Epoxies

Code	Measured Deformation Zone Size (μm)	Fracture Energy of Bulk Epoxies (kJ/m^2)	E (GPa)	$E_{substrate}$[a]/E	Locus of Failure[b]
E1	ND[c]	0.22	2.68	25.7	C
E2	ND	0.44	2.61	26.4	C
E3	ND	0.62	2.34	29.5	C
E1/CTBN13	7	0.24	2.47	27.9	C
E2/CTBN13	250	4.77	2.43	28.4	C/I
E3/CTBN13	500	7.94	2.18	31.7	I
E1/CTBN8	24	0.62	2.26	30.5	C
E2/CTBN8	200	2.64	1.98	34.8	I
E3/CTBN8	660	10.48	1.88	36.7	I

[a] 69 GPa.
[b] C, cohesive failure at TDCB fracture; I, interfacial failure at TDCB fracture.
[c] Not determined for the small size.

E2 to E3), a transition from cohesive to interfacial failure occurred, resulting in the drop of G_{Ic}.

There were several reasons why there occurred a transition from cohesive to interfacial failure with increasing M_c. One was the increase in ductility of the matrix and toughenability of matrix induced by rubber particle, which might absorb much more energy in fracture as shown in Table IV. Consequently, it appeared to prevent the crack from propagating through the adhesive layer in cohesive failure mode. Another was the formation of a weak interfacial boundary layer at the epoxy/metal interface. Figure 9(b,c), and most apparently, (f), showed that the deformation zone (rubber-cavitated zone) was confined to the substrate/epoxy interface.

An interface between two different materials has a residual stress, which results from the mismatch in elastic constants like Young's modulus or Poisson's ratio between epoxy resin and substrate.[6] As M_c increased, the modulus of the adhesive decreased, whereas that of the substrate did not change. Additionally, when the liquid rubber was added, the degree of mismatch was further enlarged. The increasing mismatch of elastic constants with increasing M_c might result in a weak interface. Consequently, crack propagation along the interface is preferred through the adhesive layer.

Still another, and more important reason for the formation of weak interface with increasing M_c, is agglomeration of rubber particles at the substrate/epoxy interface. It was noted in the specimens failed at interface [Fig. 9(b,c,f)] that there were local concentrations of the CTBN rubber particles near the interfaces. Scanning electron micrograph of the fracture surface of the TDCB specimen also shows that the agglomerated rubber-epoxy portion of several tens of micrometers bulged out on the fracture surface in interfacial failure [Fig. 10(a,b)]. Although the definite reason for the agglomeration could not be given, the following explanation could be suggested. It has been reported that the high surface energy of the metal substrate results in relatively strong interfacial secondary force interactions, and the adhesion of metal to polymer closely depends on the interfacial state of the two materials, e.g., adsorption sites or adsorption forces.[23,24] The defects, such as structural damages on the metal surfaces, might act as a seed site for attachment and growth of small molecules.[25,26] In the adhesive systems investigated, it was observed that phase separation and agglomeration is better developed at interface and the degree of agglomeration at interface was higher with larger M_c or lower AN content in CTBN. The larger rubber particles developed due to the incompatibility between the rubbers and the epoxies might not come into effective contact with metal surface. Thus, the agglomerated particles at metal/adhesive interface might act as stress concentrators and promote the development of small cracks or flaws that are located at, or near the interface. The retarded transition from cohesive to interfacial failure in the CTBN13-toughened epoxy system was considered to be attributed to better com-

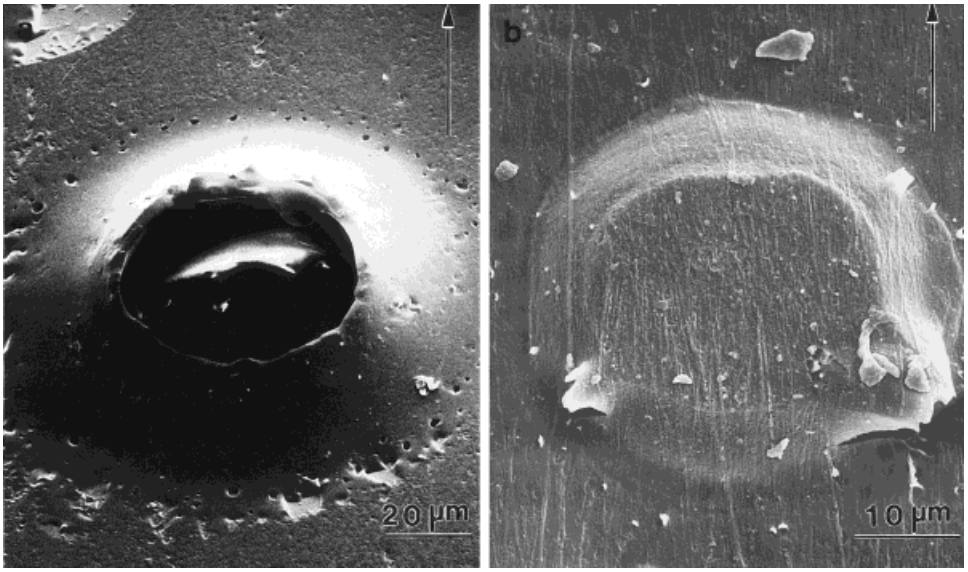

Figure 10 Scanning electron micrographs of the fracture surfaces of the TDCB specimens: (a) E3/CTBN8, and (b) E3/CTBN13. Arrows indicate the direction of crack propagation.

patibility of CTBN13 rubber with epoxy than CTBN8.

For the purpose of excluding rubber agglomeration at interface, core-shell rubber particles with predetermined size and size distribution were blended with epoxy. Compared with conventional CTBN-toughened system, in which rubber particles could directly react with epoxy matrix, a discrete interface was introduced between the particles and the epoxy matrix by the shell polymer of core-shell particles, which would not change their degree of adhesion to epoxy matrix with various M_c. As might be expected, agglomeration at the epoxy/metal interface was not observed in epoxy/

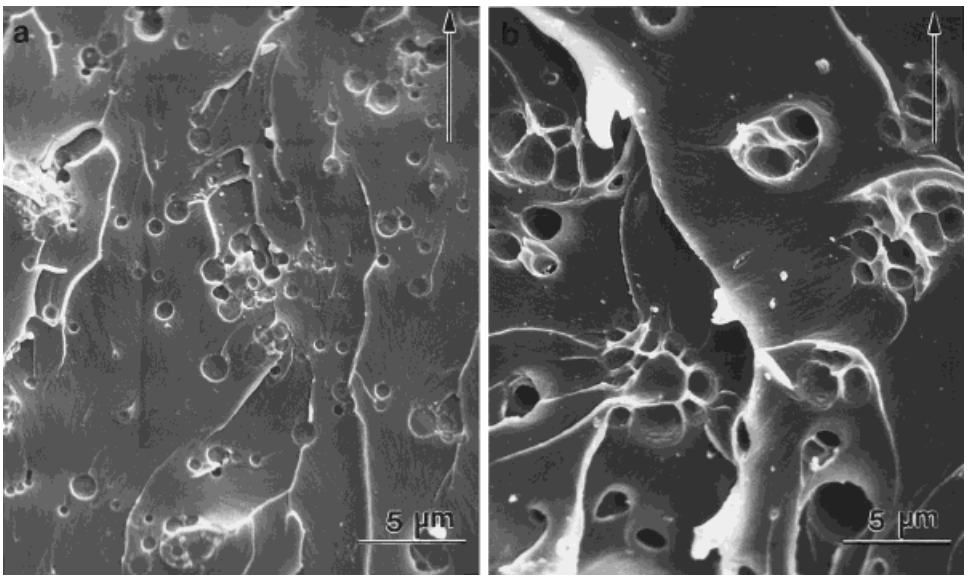

Figure 11 Scanning electron micrographs of the fracture surfaces of the TDCB specimens: (a) E1/core-shell, and (b) E3/core-shell. Arrows indicate the direction of crack propagation.

Table V Dilated Diameter of Core-Shell Particles in Fractured TDCB Specimens

Code	M_c	Dilated Diameter (nm)	Relative Dilated Diameter[a] (nm/nm)
E1	456	770	1.17
E2	1600	1250	1.89
E3	2237	1680	2.55

[a] The diameter of dilated particle/the predetermined one (630 nm).

core-shell rubber adhesive system, and all the adhesives were fractured in cohesive failure through the adhesive layer. As shown in Figure 8, fracture energy had an increasing tendency with increasing M_c, apparently due to the increasing toughenability of matrix. Scanning electron microscope of the fracture surfaces (Fig. 11) and Table V showed that the average diameter of dilated core-shell particles in E3 was approximately over two times larger than that in E1. Obviously, the results indicated that cavitation and subsequent deformation of epoxy matrix in the E3/core-shell blend [Fig. 11(b)] were much more severe than those in the E1/core-shell system [Fig. 11(a)]. It was, therefore, concluded that when rubber agglomeration at interface did not happen, the degree of epoxy/metal interfacial adhesion did not directly affect the adhesive strength, and the rubber particles played their roles in toughening. The resultant fracture energy of rubber-toughened epoxy adhesive increased with increasing M_c.

CONCLUSIONS

Fracture energy of the rubber-toughened bulk epoxy increased with M_c. However, in the CTBN-toughened adhesive system, as M_c increased, fracture behavior showed a transition from cohesive failure to interfacial failure. The transition was considered to be due to the prevention of crack from propagating cohesively by increased ductility of matrix, the formation of weak boundary by the enlarged mismatch of elastic constant, and the agglomeration of rubber particles at the metal/epoxy interface. Agglomeration at interface was thought to be the major factor determining the failure mode. Core-shell rubber toughened adhesives, which did not show the agglomeration at interface, were fractured cohesively, and fracture energy increased with increasing M_c.

REFERENCES

1. Yee, A. F.; Pearson, R. A. J Mater Sci 1986, 21, 2462.
2. Huang, Y.; Kinloch, A. J. J Mater Sci 1992, 27, 2763.
3. Bascom, W. D.; Cottington, R. L.; Jones, R. L.; Peyser, P. J Appl Polym Sci 1975, 19, 2545.
4. Wang, S. S.; Mandell, J. F.; McGarry, F. J. Int J Fracture 1978, 14, 39.
5. Hunston, D. L.; Kinloch, A. J.; Wang, S. S. J Adhes 1989, 28, 103.
6. Tvergaard, V.; Hutchinson, J. J Mech Phys Solids 1996, 44, 789.
7. Kinloch, A. J.; Shaw, S. J. J Adhes 1981, 12, 59.
8. Bell, A. J.; Kinloch, A. J. J Mater Sci Lett 1997, 16, 1450.
9. Carre, A.; Schultz, J. J Adhes 1983, 15, 151.
10. Pearson, R. A.; Yee, A. F. J Mater Sci 1989, 24, 2571.
11. Kishi, H.; Shi, Y. B.; Huang, J.; Yee, A. F. J Mater Sci 1998, 33, 3479.
12. Guthner, T.; Hammer, B. J Appl Polym Sci 1993, 50, 1453.
13. Galy, J.; Gulino, D.; Pascault, J. P.; Pham, Q. T. Makromol Chem 1987, 188, 7.
14. Ferry, J. D. Viscoelastic Properties of Polymers; John Wiley & Sons: New York, 1980.
15. Plati, E.; Williams, J. G. Polym Eng Sci 1975, 15, 470.
16. Mostovoy, S.; Ripling, E. J. J Appl Polym Sci 1966, 10, 1357.
17. Pearson, R. A.; Yee, A. F. J Mater Sci 1991, 26, 3828.
18. Holik, A. S.; Kambour, R. P.; Hobbs, S. Y.; Fink, D. G. Microstruct Sci 1979, 16, 357.
19. Wang, T. T.; Zupko, H. M. J Appl Polym Sci 1981, 26, 2391.
20. Chen, T. K.; Jan, Y. H. J Mater Sci 1992, 26, 111.
21. Rowe, E. A.; Siebert, A. R.; Drake, R. S. Mod Plast 1970, 47, 110.
22. Verchere, D.; Pascault, J. P.; Sautereau, H.; Moschiar, S. M.; Riccardi, C. C.; Williams, R. J. J. Polymer 1989, 30, 107.
23. Kinloch, J. Adhesion and Adhesives: Science and Technology; Chapman and Hall: New York, 1987, Chapter 3.
24. Minford, J. D. In Treatise on Adhesion and Adhesives; Patrick, R. L., Ed.; Marcel Dekker: New York, 1973, Chapter 2, Vol. 3.
25. Jackson, S. T.; Friends, A. D.; Wool, R. P. Polym Prepr 1993, 34, 300.
26. Lewis, A. F. In Epoxy Resins: Chemistry and Technology; May, C. A., Ed.; Marcel Dekker: New York, 1988, Chapter 7.